# Gramicidin A Aggregation in Supported Gel State Phosphatidylcholine Bilayers†

Jianxun Mou, Daniel M. Czajkowsky, and Zhifeng Shao*

*Department of Molecular Physiology & Biological Physics and Biophysics Program, University of Virginia Health Sciences Center, Box 449, Charlottesville, Virginia 22908*

*Received August 24, 1995; Revised Manuscript Received January 3, 1996*⊗

ABSTRACT: Using an atomic force microscope, supported bilayers of saturated phosphatidylcholine (in the gel state) containing various amounts of gramicidin A (gA) were imaged in aqueous solutions and at room temperature. gA clusters were directly observed for the first time under these conditions. It was found that, at a lower gA concentration, gA aggregated into domains, composed of small clusters along with a considerable amount of lipids. This basic aggregation unit, most likely a hexamer, remained the same for acyl chain lengths from 14 to 18 carbons. These small clusters were observed to form elongated aggregates (line type) but never into extended pure gA domains. When gA concentrations were increased, for bilayers with 16 carbons or less, gA aggregated into larger domains but the basic unit remained separated by lipid molecules. At about 5 mol % gA, a percolation-like transition occurred at which the line type aggregates were connected to each other. However, for bilayers with more than 16 carbons, multiple lamellar strucutres were formed at higher gA fractions and the top layer had a ripple-like surface morphology. The molecular mechanism for the formation of these peculiar structures remains to be elucidated.

The small channel-forming peptide, gramicidin (gr), has been one of the most extensively studied peptides via various biophysical and biochemical methods (Busath, 1993; Killian, 1992; Wooley & Wallace, 1992). The interest in this pentadecapeptide stems mostly from its relatively simple structure, now known at the atomic resolution (Arseniev et al., 1985; Ketchem et al., 1993; Langs, 1988), which could provide useful insight into the mechanism of ion channel functions in general (Hille, 1992). On the basis of solid state NMR (Hu et al., 1993; Ketchem et al., 1993; Prosser et al., 1994) and other techniques (Hing et al., 1990; Langs, 1988; Katsaras et al., 1992), it has been established that gr forms a $\beta$-helix spanning a single leaflet of the bilayer. Through N−N dimerization with one gr residing in the hydrocarbon region of each leaflet, a small ion channel across the bilayer can be formed which is cation selective (Krasne et al., 1971; Urry, 1971; Wooley & Wallace, 1992; Urry et al., 1971). The function of gr as an ion channel in the bilayer is now considered to be well-understood, with many models describing the ion movement in the lumen of the channel (Roux & Karplus, 1994; Roux et al., 1995).

In addition to the atomic structure, the aggregation state of gr in lipid bilayers is also of great interest (Killian, 1992), although the results so far are not conclusive due to the limitations of the techniques available. For example, when gr was incorporated in phosphatidylcholine bilayers, a two-phase (gel and fluid) coexistence was found for gr mole fractions below 2%. Above this fraction, a continuous phase was found, implying that gr could be uniformly distributed (Morrow & Davis, 1988). In another study, it was suggested that gr became highly aggregated only above 6 mol % in the gel state DPPC[1] bilayer (Killian & Kruijff, 1985; Chapman et al., 1977). However, a more recent study suggests that, at least for fluid DLPC bilayers, gr is uniformly distributed up to 10 mol % (He et al., 1993). When gr was mixed with lysophosphatidylcholine, freeze-fracture electron microscopy revealed elongated aggregations of gr at mole fractions up to 11% (Spisni et al., 1983). In this study, it was suggested that the elongated aggregation is composed of distinct basic units of gr hexamers with a diameter of 3−4 nm, although such a basic unit was not directly resolved.

In this report, we present the results of atomic force microscopy (AFM) studies of gramicidin A (gA) in gel state phosphatidylcholine bilayers in aqueous solutions and at room temperature. With supported bilayers containing different mole fractions of gA, the aggregation of gA is directly observed by AFM. The resolution is sufficient to resolve isolated monomers and larger oligomers. The morphology of such bilayers is surprising: there are "point-like" and elongated clusters of gA, both of a similar lateral dimension, consistent with the proposed hexamer model (Spisni et al., 1983). The domains with aggregated gA contain a large amount of lipid which is thicker than a normal bilayer. A discussion of the AFM observation in relation to the existing models will also be presented.

## MATERIALS AND METHODS

*Materials.* Synthetic phosphoplipids, dimyristoyl- (DMPC), dipentadecanoyl- (diC15-PC), dipalmitoyl- (DPPC), diheptadecanoyl- (diC17-PC), and distearoylphosphatidylcholine (DSPC), were obtained from Avanti Polar Lipids (Alabaster, AL) or Sigma Chemicals (St. Louis, MO) and were used

† This work was supported by grants from National Institutes of Health (RO1-RR07720 and PO1-HL48807) and National Science Foundation (BIR-9115655).

* To whom correspondence should be addressed.

⊗ Abstract published in *Advance ACS Abstracts,* February 15, 1996.

[1] Abbreviations: AFM, atomic force microscopy; gA, gramicidin A; DLPC, dilauroylphosphatidylcholine; DMPC, dimyristoylphosphatidylcholine; diC15-PC, dipentadecanoylphosphatidylcholine; DPPC, dipalmitoylphosphatidylcholine; diC17-PC, diheptadecanoylphosphatidylcholine; DSPC, distearoyl phosphatidylcholine.

0006-2960/96/0435-3222$12.00/0 

without further purification. The purity was better than 99% according to the manufacturers. Gramcindin A (gA) was obtained from Calbiochem Biochemicals (La Jolla, CA) with purity higher than 99%. No further purification was performed. All other chemicals were of reagent grade and were obtained from Sigma Chemicals.

*Specimen Preparation*. The appropriate amount of gA in trifluoroethanol was first mixed with phospholipids in chloroform at a predetermined molar ratio. After the solvents were completely evaporated under dry nitrogen, the mixed powder was resuspended in 20 mM NaCl at a concentration of 0.5−1 mg/mL. Unilamellar vesicles were made with repeated sonication in an ultrasonic cleaning bath where the temprature was controlled to below 45 °C. A small droplet of the vesicle solution was applied to a freshly cleaved mica surface at room temperature. After incubation at 4 °C for up to 10 h, excess solution was washed off with 20 mM NaCl. Supported unilamellar bilayers were formed when such prepared specimens were heated up to 60 °C for 30 min. To ensure the integrity of the bilayer, the specimen was never exposed to air.

*Atomic Force Microscopy*. AFM has been shown to be an effective method for studying soft biological materials in aqueous buffers (Shao & Yang, 1995; Hansma & Hoh, 1994). The reproducibility and the validity of AFM for studying supported bilayers have already been documented elsewhere (Mou et al., 1995; Hui et al., 1995; Yang et al., 1993). In this study, all images were obtained with a NanoScope II AFM (Digital Instruments, Santa Barbara, CA) with a homemade fluid cell in the contact mode. The scanner was calibrated with a gold ruling of known dimensions. The cantilevers had a nominal spring constant of 0.06 N/m with an integrated oxide-sharpened pyramid tip (Digital Instruments). The scanning speed was typically 7 Hz, and the typical probe force was 0.5−1 nN. All images are the original data without filtering.

## RESULTS

Without gA, supported phosphatidylcholine bilayers have a flat appearance under AFM in solution. As an example, a DPPC bilayer is shown in Figure 1a, where some bilayer defects are also present (darker areas). The thickness of the DPPC bilayer, measured from the edge of these defects, is 5.6 ± 0.3 nm ($n = 60$). For DSPC bilayers (DSPC has 2 more carbon atoms in each acyl chain than DPPC), the thickness measured with AFM is 6.9 ± 0.5 nm ($n = 60$). At a higher resolution, no heterogeneity in thickness was observed, and individual head groups of the lipids were not resolved by AFM in these gel state bilayers, consistent with previous observations (Mou et al., 1994, 1995). When 1 mol % gA was incorporated into a DPPC bilayer, the surface remained largely planar, but line type depressions, 3.7 ± 0.7 nm wide and 0.5 ± 0.1 nm deep, were observed sparsely distributed in the bilayer. Small pointlike depressions with diameters varying from 3 to 5 nm were also observed (see Figure 1b). Inasmuch as gA primarily resides in the hydrocarbon core (Ketchem et al., 1993), they are expected to appear as surface depressions in a bilayer when imaged with AFM.

When the gA fraction was increased to 2 mol %, an interesting aggregation pattern emerged in the DPPC bilayer (Figure 2). At a large scale, it was found that gA aggregated into domains of variable shape and size (see Figure 2a). At a higher resolution, such gA rich domains contained both the line type and the pointlike gA aggregates and a considerable amount of lipid separating the gA aggregates (see Figure 2b). It is also noted that the line type aggregates changed direction in a random fashion, but with a somewhat regular length before each bend. The measured segment length is 13 ± 8 nm. The line type gA aggregates, although occupying a substantial area of the gA rich domains, are not all connected, and on average, the diameter of the pointlike aggregates was similar to the width of the line type gA aggregates. Furthermore, the thickness of the lipid bilayer between the gA aggregates was slightly greater than those in the gA free region (see Figure 2b inset). The exact

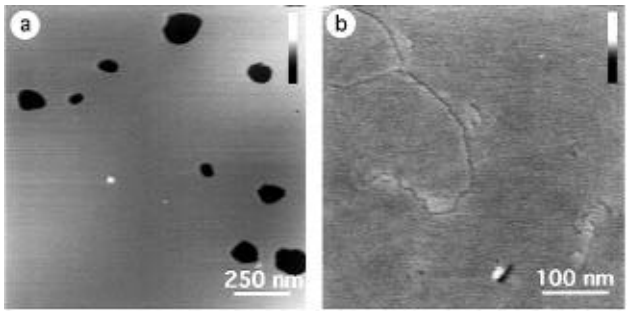


FIGURE 1: AFM images (contact mode) of supported membranes on a mica surface in 20 mM NaCl, obtained at room temperature. (a) A DPPC bilayer is shown with many defects (darker areas). From these defects, the thickness of the bilayer was measured as 5.6 nm, consistent with previous measurments (Mou et al., 1994) if a thin layer of solution, normally 1−2 nm, between the bilayer and the mica surface is taken into account (Tamm & McConnell, 1985). Without gA, the bilayer surface appeared relatively flat without details. Individual head groups were not resolved by the AFM. The height scale is 20 nm. (b) When 1 mol % gA was mixed with DPPC, both pointlike clusters (arrows) and elongated aggregates (as surface depressions) were observed. The lateral dimensions of these clusters were about the same (∼3−4 nm). Since gA primarily resides in the hydrocarbon core, they should appear as depressions of the surface. The height scale is 6 nm.

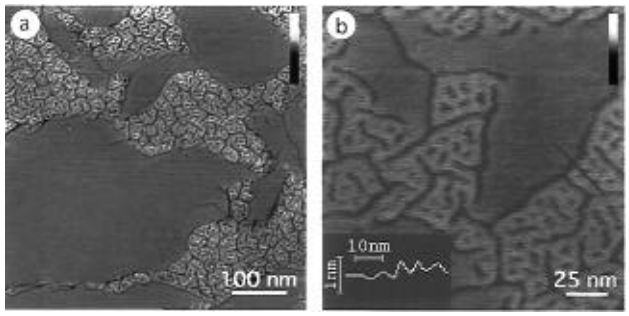


FIGURE 2: AFM images showing gA aggregation at 2 mol % in DPPC. (a) At a lower resolution, gA was seen aggregated into domains, and both the elongated aggregates and pointlike clusters were present, in an apparent equilibrium. Note that gA aggregates appear as surface depressions (dark regions) in the bilayer. The height scale is 5 nm. (b) At a higher resolution, these gA aggregates were well-resolved. The width of these aggregates is the same as that at a lower gA mole fraction. At the boundary of the gA rich domains, elongated aggregates are more abundant, and within the gA rich domains, a considerable amount of lipid is present, separating the basic seggregation units (clusters) of gA. The distance between the gA aggregates was also about the same. Within these regions, the membrane also appeared thicker than that without gA. The elongated aggregates are not connected at this gA fraction. The height scale is 5 nm. The scan profile along the line indicated in b is shown in the inset.

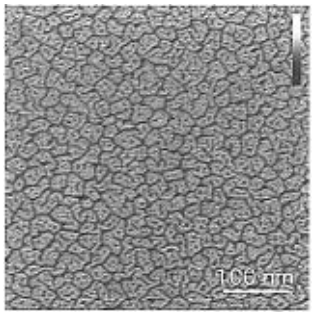

FIGURE 3: At 5 mol % gA in a DPPC bilayer, the membrane morphology went through a percolation type transition; almost all elongated aggregates are now connected, although isolated pointlike gA clusters can still be found, trapped between the elongated gA boundaries. Even at this fraction, the lateral dimension of the gA aggregates remained the same, supporting the suggestion that there is a dominant gA cluster (basic aggregation unit) in DPPC bilayers which can only associate in one dimension. Furthermore, when these units were connected, tristar-like joints are seen, perhaps reflecting the molecular arrangement of the gA basic (aggregation) unit. The height scale is 4 nm.

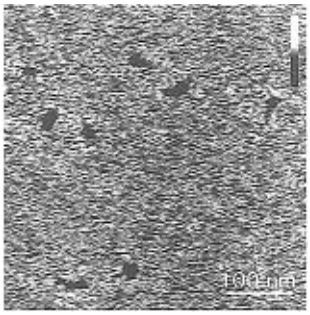

FIGURE 4: At 10 mol %, the morphology of the bilayer became difficult to describe. There were no longer clearly separated domains. However, even at this high gA fraction, extended gA domains were never observed and the membrane still remained planar on the mica surface. Some bilayer defects are also seen (dark areas). The height scale is 10 nm.

organization of these lipids cannot be determined by AFM due to its limited resolution.

As the gA mole fraction was increased further in a DPPC bilayer, the gA rich domains continued to grow. At about 5 mol % gA, the entire bilayer had a uniform appearance, but gA never phase separated into extended domains (Figure 3). Instead, a considerable amount of lipids was retained between the pointlike and line type gA aggregates. At this gA fraction, the line type gA aggregates are all interconnected, and it appears that most of the gA is in the line type aggregates. The total bilayer surface occupied by gA is about 24%, which agrees well with what is expected with 5 mol % gA in the bilayer, if the diameter of the gA cross section is 1.7 nm (Ketchum et al., 1993). At 10 mol % gA, the distinction between the gA domains and lipid domains disappeared (Figure 4), but the surface morphology is very different from that of a planar bilayer (see Figure 1a). In this case, the distribution and aggregation of gA and lipids cannot be inferred from these images.

The measured diameter of the gA aggregates (pointlike) from these images is shown in Figure 5a, with a mean value of 3.7 nm. The measured width of the line type aggregates (Figure 5b) yielded exactly the same value. Interaggregate distance was also measured with these samples and is shown in Figure 5c. It is clear that this distance also fell into a fairly narrow region (4−6 nm), and the mean value is 4.6 ± 0.8 nm. Similar results were also obtained with gel state DMPC bilayers, although the contrast was much lower, perhaps because of the smaller thickness of a DMPC bilayer (Janiak et al., 1979). However, the aggregation state of gA appeared the same, despite the shorter length of the acyl chains of DMPC. Nearly identical results were also obtained with diC15-PC bilayers. The "critical" fraction for the percolation transition was about the same for these lipids.

Interestingly, the aggregation behavior of gA changed with longer acyl chain phosphatidylcholines. With bilayers of diC17-PC and DSPC (diC18-PC), gA aggregation was also observed and the bilayer remained in the planar form at low gA fractions. In Figure 6a, a diC17-PC bilayer containing 2 mol % gA is shown. The small aggregates had a dimension similar to that with shorter acyl chains, i.e., DPPC, diC15-PC, and DMPC. However, the fraction of aggregates in the elongated line type clusters is much higher, although the width of these line type aggregates is about the same. Similar results were also obtained with bilayers of DSPC at gA concentrations below 2 mol %. However, when the gA fraction was increased to 5 mol %, the bilayer morphology changed significantly. Rather than unilamellar bilayers, multiple lamellar structures were formed on the mica surface with both diC17-PC and DSPC. An example is shown in Figure 6b, where the specimen was prepared with diC17-PC containing 5 mol % gA. Most of the samples had a double layer structure; a ripple-like surface was observed on the top layer, while the lower layer had a morphology similar to that in Figure 6a. The periodicity of these ripples is 10.6 nm. On the basis of the AFM images alone, we cannot determine whether these were gA aggregates or

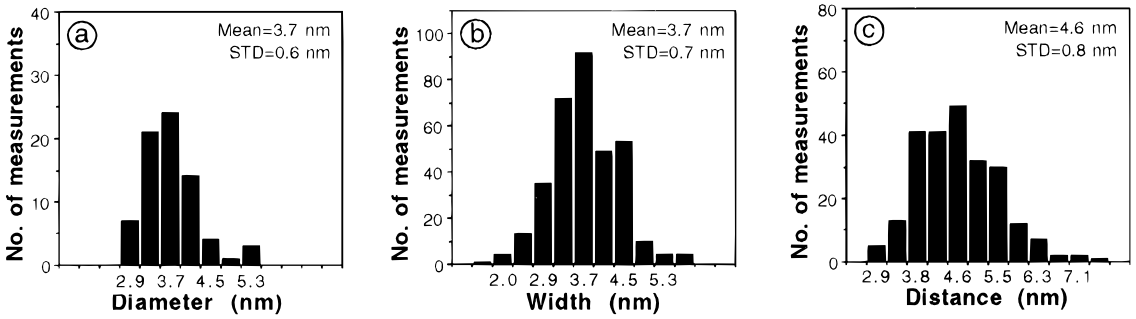


FIGURE 5: (a) Histogram for the measured diameter of the gA aggregates (pointlike) in DPPC bilayers at different concentrations. The mean value is 3.7 nm with a standard deviation of 0.6 nm. (b) Histogram for the measured width of elongated gA aggregates (line type) in the same bilayers. The mean value is exactly the same as that for the pointlike aggregates. (c) Histogram for the distance between gA aggregates. In these measurements, when a pointlike aggregate was trapped in a line type aggregate boundary, the shortest distance was measured. The mean value is 4.6 nm.

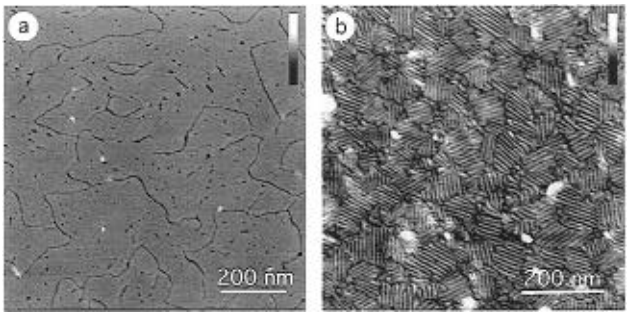


FIGURE 6: AFM images of gA aggregation in diC17-PC bilayers. (a) At a 2 mol % gA concentration, similar gA aggregates were observed, although the elongated aggregates were more predominant, which is different from that of the thinner bilayers. Surprisingly, the lateral dimension of these aggregates was essentially the same as in the other bilayers, although the bilayer thickness near gA aggregates was not as different as with other lipids. The height scale is 6 nm. (b) However, at 5 mol % gA, the bilayer morphology was drastically different from those observed with DPPC. Multiple lamellar structures (primarily double layers) were observed; the upper layer had a ripple-like surface, but the lower layer appeared the same as that at 2 mol % gA. These layers did not appear coupled to each other. Shown here is the surface of the topmost bilayer. The height scale is 6 nm.

bilayer undulations. However, it is clear that gA must have played a role in the formation of this structure.

Unfortunately, attempts to image gA in fluid state bilayers were not successful, due to the low contrast where the bilayer was too compressible. As a result, gA molecules could not be detected by AFM unambiguously at room temperature.

## DISCUSSION

*(1) There Is a Basic gA Aggregation Unit.* On the basis of the AFM images of these five types of saturated phosphatidylcholines at low gA fractions, a basic aggregation unit (pointlike) of gA can be inferred. The diameter of this basic unit is 3.7 nm, as measured by AFM with a relatively small standard deviation (Figure 5a). Since this was observed in all of the bilayers (with a chain length from 14 to 18 carbons), it strongly suggests that the size of the basic unit is primarily determined by the intrinsic properties of gA. This is somewhat surprising, because it was suggested that 16-carbon acyl chains were the optimal length and that any mismatch in the hydrocarbon region could lead to phase separation (Watnick & Chan, 1990). It is rather peculiar to note that these basic units can only associate to form elongated line type aggregates (see Figure 2) with a nominal width similar to the diameter of the basic unit (3.7 nm; see Figure 5b). No other types of aggregates were observed in these samples. We do not have an explanation for why two-dimensional growth of the gA aggregates is not favored in these gel state bilayers. It appears that at gA fractions less than 1% the line type aggregates are more favorable than isolated pointlike basic units, and for longer chain lipids ($>16$), this preference is further enhanced even at a gA fraction of 2% (see Figure 6). The mechanism for the coexistence of two morphologically different aggregates is not understood. However, it is clear that microaggregation, i.e., the basic unit, already occurred at very low gA fractions. These observations seem to suggest that the previously inferred gA aggregation based on thermodynamic studies was the association or rearrangement of these basic units, rather than the aggregation of gA monomers.

The dimensions determined by AFM for the basic aggregation unit are consistent with a previous suggestion that a hexamer of gA is the smallest aggregation cluster, which was inferred from electron microscopical observations of gA in lysophosphatidylcholine bilayers (Spisni et al., 1983). However, due to the relatively large size of the atomic force microscope tip (5−10 nm raduis of curvature at the apex) (Albretch et al., 1993), the lateral dimension of these basic units could be underestimated, because the surface of the gA is below the surface of a bilayer.[2] Therefore, the possibility of more than 6 gA monomers in a basic unit cannot be entirely ruled out.

*(2) Percolation Transition for PC Bilayers with 16 Carbons or Less*. A striking feature upon the gA fraction being increased is that at about 5 mol % the morphology of gA aggregation drastically changed; a large proportion of gA aggregates was interconnected (see Figure 3). However, the lateral dimension of the gA aggregates remained the same as that at lower gA fractions. The pointlike basic units were still apparent and trapped in between the line type aggregates. The complicated pattern of these aggregates suggests that the line type aggregates have percolated (all connected) around this gA concentration. Such a large scale structural transition seems to correspond to the previously described onset aggregation at about 6 mol % gA in DPPC bilayers (Killian & Kruijff, 1985; Chapman et al., 1977). It is also interesting that the angles between adjoining aggregate arms were more or less 120°, which may actually reflect the arrangement of gA monomers within the basic unit. Unfortunately, AFM was unable to resolve such finer details on these specimens. An elucidation of the underlying principles governing this aggregational transition may provide useful information about the lipid−peptide interaction.

*(3) The Bilayer Surface Is Modified between gA Aggregates*. As revealed in Figure 2 and 3, when gA aggregated into distinct domains at low concentrations, the lipid bilayer enclosed by the gA aggregates appeared thicker than that outside these regions. Furthermore, the distance between gA aggregates remained roughly the same over large areas. A histogram of this measurement is shown in Figure 5c. These observations suggest that, in the gA rich domains, a complex molecular assembly is formed in which the lipid arrangements are not the same as that in a normal bilayer. It can be inferred that the bilayer surface between gA aggregates is no longer flat, which is consistent with a previous theoretical study (Huang, 1986), where the surface curvature was predicted to change due to the presence of gA. This observation is also consistent with the suggestion that the state of lipids could be different depending on whether they are in contact with the peptide (Muller et al., 1995; Rice & Oldfield, 1979; Pink et al., 1981). At about 5 mol %, almost all of the lipids appeared to associate with gA clusters, and the entire bilayer was transformed into a single molecular complex, the same as that in gA rich domains at lower gA fractions. We must also point out that the characteristic distance between gA aggregates has not been predicted by the theories describing the behavior of peptides in a bilayer (Pearson et al., 1984; Mouritsen & Bloom, 1993). If we assume that a certain number of lipids were tightly bound with each gA aggregation unit, it would not be consistent

[2] For structures protruding from the surface, the opposite would be true.

with the existence of the line type aggregates in these bilayers. We have also noticed that, when a single gA unit is surrounded by the line aggregates (trapped), it was located at a particular distance close to the line aggregates, but not at the center. This observation indicates that the energy is at the lowest when these gA aggregates are separated at this distance (∼4.6 nm).

*(4) Effect of High gA Concentrations on Bilayer Morphology*. For bilayers of acyl chains with more than 16 carbons, multiple lamellar structures were preferentially formed with 5 mol % gA. However, the distribution of gA in these multiple layers did not appear the same. More interestingly, the top layer always had a ripple-like structure. It is not clear at present whether the difference in structure is caused by the substrate interaction. It is clear that the ripple-like structure was induced by the gA in the bilayer, because, without gA, multiple bilayers were rarely formed. However, these ripple-like structures could not be identified as the $H_{II}$ phase (Killian & Kruijff, 1988) for several reasons. First, the width of the ripples is about 10.6 nm, much larger than the 7 nm tubes reported previously (Killian & Kruijff, 1988). Second, the layers did not appear interconnected. When a larger probe force was used, the top layer could be easily scraped away, exposing the lower layer which appeared the same as those with low gA concentrations (Figure 6a). In other words, the two layers do not have the same surface structure. Since no adhesion force was observed on the lower layer surface, it must be a bilayer, because an adhesion force was shown present when hydrophobic surfaces were imaged with these cantilevers (i.e., the lower layer was not an exposed monolayer). On the basis of these results, the observed structure on the top layer could be an intermediate state between the lamellar phase and the $H_{II}$ phase. Further study with other techniques will be required to solve this problem.

In conclusion, we have demonstrated that AFM is one of the preferred methods for studying membrane structures under nearly native conditions. A basic gA aggregation unit, most likely a hexamer, was directly resolved by AFM for the first time, and the behavior of these micro-gA clusters aggregating into larger domains in gel state phosphatidylcholine bilayers was elucidated. The rather constant size of the gA basic unit in different chain length bilayers strongly suggests that such clusters are determined by the intrinsic gA−gA interactions. An aggregational transition (percolation) at ∼5 mol % gA was also found for the first time in bilayers with 16 carbons or less, providing a direct explanation of the previously observed gA aggregation at ∼6 mol % with other techniques; i.e., it is the rearrangement of the gA basic units rather than the aggregation of gA monomers.

## ACKNOWLEDGMENT

We thank Yiyi Zhang and Gang Huang for technical assistance. We also thank Professor A. P. Somlyo for encouragement.

## REFERENCES

Albrecht, T. R., Akamine, S., Carver, T. E., & Quate, C. F. (1990) *J. Vac. Sci. Technol. A8*, 3386−3396.
Arseniev, A. S., Barsukov, I. L., Bystrov, V. F., Lomize, A. L., & Ouchinnikov, Yu. A. (1985) *FEBS Lett. 186*, 168−174.
Busath, D. D. (1993) *Annu. Rev. Physiol. 55*, 473−501.
Chapman, D., Cornell, B. A., Eliasz, A. W., & Perry, A. (1977) *J. Mol. Biol. 113*, 517−538.
Hansma, H. G., & Hoh, J. (1994) *Annu. Rev. Biophys. Biomol. Struct. 23*, 115−128.
He, K., Ludtke, S. J., Wu, Y., & Huang, H. W. (1993) *Biophys. J. 64*, 157−162.
Hille, B. (1992) *Ionic Channels of Excitable Membranes*, Sinauer Associates, Sunderland, MA.
Hing, A. W., Adams, S. P., Silbert, D. F., & Norberg, R. E. (1990) *Biochemistry 29*, 4156−4166.
Hu, W., Lee, K.-C., & Cross, T. A. (1993) *Biochemistry 32*, 7035−7047.
Huang, H. W. (1986) *Biophys. J. 50*, 1061−1070.
Hui, S. W., Viswanathan, R., Zasadzinski, J. A., & Israelachvili, J. N. (1995) *Biophys. J. 68*, 171−178.
Janiak, M. J., Small, D. M., & Shipley, G. G. (1979) *J. Biol. Chem. 254*, 6068−6078.
Katsaras, J., Prosser, R. S., Stinson, R. H., & Davis, J. H. (1992) *Biophys. J. 61*, 827−830.
Ketchem, R. R., Hu, W., & Cross, T. A. (1993) *Science 261*, 1457−1460.
Killian, J. A. (1992) *Biochim. Biophys. Acta 1113*, 391−425.
Killian, J. A., & de Kruijff, B. (1985) *Biochemistry 24*, 7881−7890.
Killian, J. A., & de Kruijff, B. (1988) *Biophys. J. 53*, 111−117.
Krasne, S., Eisenman, G., & Szabo, G. (1971) *Science 174*, 412−415.
Langs, D. A. (1988) *Science 241*, 188−191.
Morrow, M. R., & Davis, J. H. (1988) *Biochemistry 27*, 2024−2032.
Mou, J., Yang, J., & Shao, Z. (1994) *Biochemistry 33*, 4439−4443.
Mou, J., Yang, J., & Shao, Z. (1995) *J. Mol. Biol. 248*, 507−512.
Mouritsen, O. G., & Bloom, M. (1993) *Annu. Rev. Biophys. Biomol. Struct. 22*, 145−171.
Muller, J. M., van Ginkel, G., & van Faassen, E. E. (1995) *Biochemistry 34*, 3092−3101.
Pearson, L. T., Edelman, J., & Chan, S. I. (1984) *Biophys. J. 45*, 863−871.
Pink, D. A., Georgallas, A., & Chapman, D. (1981) *Biochemistry 20*, 7152−7157.
Prosser, R. S., & Davis, J. H. (1994) *Biophys. J. 66*, 1429−1440.
Prosser, R. S., Daleman, S. I., & Davis, J. H. (1994) *Biophys. J. 66*, 1415−1428.
Rice, D., & Oldfield, E. (1979) *Biochemistry 18*, 3272−3279.
Roux, B., & Karplus, M. (1994) *Annu. Rev. Biophys. Biomol. Struct. 23*, 731−761.
Roux, B., Prod'hom, B., & Karplus, M. (1995) *Biophys. J. 68*, 876−892.
Shao, Z., & Yang, J. (1995) *Q. Rev. Biophys. 28*, 195−251.
Spisni, A., Pasquali-Ronchetti, I., Casali, E., Lindner, L., Cavatorta, P., Masotti, L., & Urry, D. W. (1983) *Biochim. Biophys. Acta 732*, 58−68.
Tamm, L. K., & McConnell, H. M. (1985) *Biophys. J. 47*, 105−113.
Urry, D. W. (1971) *Proc. Natl. Acad. Sci. U.S.A. 68*, 672−676.
Urry, D. W., Goodall, M. C., Glickson, J. D., & Mayers, D. F. (1971) *Proc. Natl. Acad. Sci. U.S.A. 68*, 1907−1911.
Watnick, P. I., & Chan, S. I. (1990) *Biochemistry 29*, 6215−6221.
Wooley, G. A., & Wallace, B. A. (1992) *J. Membr. Biol. 129*, 109−136.
Yang, J., Tamm, L. K., Tillack, T. W., & Shao, Z. (1993) *J. Mol. Biol. 229*, 286−290.

BI9520242